



# Improving of Mixing Efficiency in a Stirred Reactor for Lead Recycling Using Computer Simulation

*Pedro VITE-MARTINEZ<sup>1)</sup>, Adán RAMÍREZ-LÓPEZ<sup>2)</sup>, Antonio ROMERO-SERRANO<sup>3)</sup>, Federico CHÁVEZ-ALCALÁ<sup>4)</sup>, Simón LÓPEZ-RAMÍREZ<sup>5)</sup>*

<sup>1)</sup> Instituto Politécnico Nacional (IPN-SEPI-ESIQIE), Metallurgical Engineering P. B. Edif. Z and Edif. 6 C.P. 07300, México City, México

<sup>2)</sup> Instituto Tecnológico Autónomo de México (ITAM), Departamento académico de ingeniería Industrial y operaciones, Mexico City, México

<sup>3)</sup> Instituto Politécnico Nacional (IPN-SEPI-ESIQIE), Metallurgical Engineering P.B. Edif. Z and Edif. 6 C.P. 07300, México City, México

<sup>4)</sup> Instituto Politécnico Nacional (IPN-SEPI-ESIQIE), Metallurgical Engineering P.B. Edif. Z and Edif. 6 C.P. 07300, México City, México

<sup>5)</sup> Instituto Politécnico Nacional (IPN-SEPI-ESIQIE), Metallurgical Engineering P.B. Edif. Z and Edif. 6 C.P. 07300, México City, México

DOI: 10.29227/IM-2015-01-05

## Summary

*Recycling is helping to reduce environmental risks and damages. Liquid lead is recovered from batteries in stirred batch reactors. Nevertheless it is necessary to establish parameters to evaluate mixing performance in order to make more efficient the industrial practices. Then this work is dedicated to simulate fluid hydro-dynamics in a lead stirred reactor by monitoring the distribution of an injected tracer to find the best injection point. Different injected points have been evaluated monitoring the tracer concentration on a group of points inside the batch to verify mixing. The tracer is assumed as ideal (with the same physical properties than lead). The reactor is a batch with two geometrical sections one cylindrical body and a semispherical on the bottom. The impeller used to promote lead stirring is a shaft with four flat blades. The tracer concentration on the monitoring points is averaged to evaluate the efficiency all around the reactor. Finally invariability of tracer concentration on the monitoring points is adopted as the criterion to evaluate mixing.*

*Keywords: lead stirring, mixing efficiency evaluation, tracer concentration, computational fluid dynamics (CFD)*

## Introduction

Lead is a dangerous metal for environment. Lead and sulphuric acid are presented in vehicle batteries; which are electrochemical devices used to store energy generated using a cell with a cathode and an anode submerged in an electrolytic solution. Nevertheless these components are toxic and corrosive, these can cause contamination of the air, soil and water; and can also be cause for an explosion or a fire. Moreover exposure to these components can produce serious health hazard to humans and natural life. Although lead-acid batteries can be recharged many times; its working life is limited. Batteries are the most popular products where lead is presented. Lead is collected to be recycled not only to reduce environmental damages. Recycling process uses less energy than refining primary ore. Nowadays, recycling has become in a clean-economical alternative for many industrial trials. This fact is a motivation for improving the industrial lead processing. The evaluation of mixing performance is very important in order to reduce working times and increase the stirring efficiency. Stirring in

chemical reactors is a complex problem to be simulated. Some authors have been working on lead recycling. But the geometrical configuration of the reactors and the operating conditions are different for each case. Some authors as Kohl and Xantidis (1999), simulated lead bullion in hemispherical vessels known as kettles. Other authors as Bailey et al. (1999), have been working studying fluid flow dynamics in reactors for different purposes such as resin beads and scaling-up. But hydrodynamic behavior and physical properties are particular for each situation simulated. The knowing of hydrodynamics phenomena is very important to improve actual practices. Zhong and Guanrong (2008) studied the effect of perturbations in stirred tanks. Others as Feng et al. (2007) have analyzed chemical reactions and the evolution of liquid-liquid phases. In the present work, geometrical configuration of lead reactor was built computationally using real industrial data. Simulation of the hydrodynamics fluid flow is done using the software Fluent (6.0); and the results of the tracer concentration on each monitoring node are saved at every step time ( $t+\Delta t$ )

on independent files to be graphed and treated using Microsoft Excel to evaluate mixing efficiency as a function of the time.

### Geometrical Model (Reactor)

The industrial reactor analyzed is sectioned in two parts. The first is the main body with a cylindrical form and a semispherical section on the bottom as is shown in Figure 1. The cylindrical diameter is 0.44 m. and it is 0.470 m. high. The reactor is symmetrical for vertical axis. Here a triangular mesh using a two dimensional model is defined for discretization. These walls are also declared as free of defects and friction. The mesh used for discretization is no structured. It was selected for a better fit with cylindrical and semi-spherical geometries of the reactor.

### Geometrical Model (propeller)

The industrial reactor is stirred using a propeller. This is formed with a main vertical shaft and two

rectangular flat solids intersected in the vertical shaft as is shown in Figures 2a and 2b. The shaft is 0.610 m. length enough to be placed inside the reactor. The propeller is formed with four rectangular blades which are placed symmetrically each  $90^\circ$ . Shaft and blades are formed by three solids united in one single body. Here, again a mesh with triangular and tetragonal cells is used for discretization.

### Geometrical Model (Fluid Domain)

The lead bulk volume inside the reactor is obtained with an inverse geometrical operation. The volume is rest from the original volume between the walls minus the propeller volume. The smallest cells are placed near the propeller and the biggest cells are near the wall reactor due to the lead volumes inside the reactor are in contact with the propeller.

### Initial assumptions

The following assumptions and boundary condi-

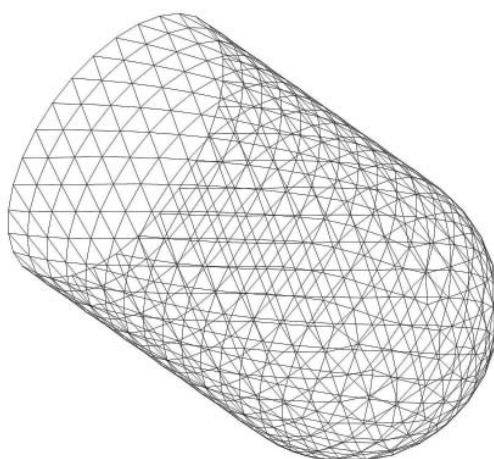


Fig. 1..Geometrical model isometric and two dimensional views (reactor)  
Rys. 1. Izometryczny model geometryczny i dwuwymiarowy widok (reaktor)

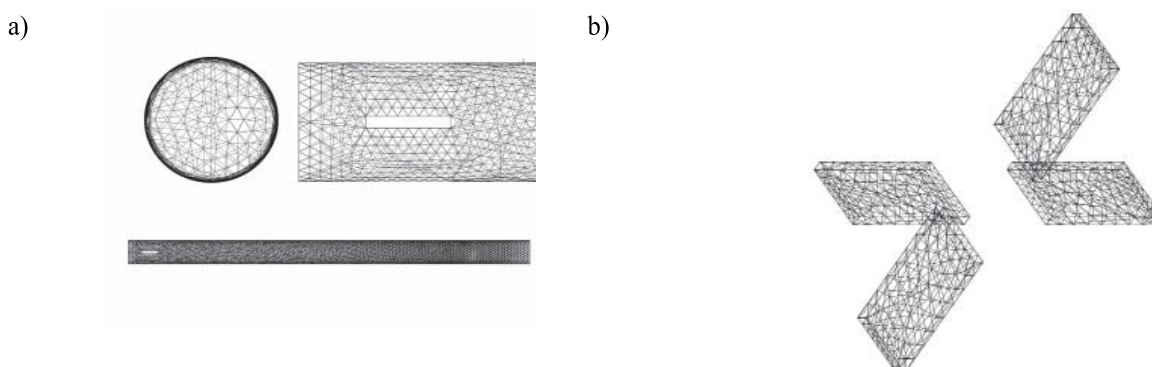


Fig. 2. Geometrical model impeller a) shaft mesh; b) Views of the four blades meshed  
Rys. 2. Model geometryczny wirnika a) siatka wału; b) widok czterech zazębionych ostrzy

tions are taken in count for all the simulation exposed on this work.

- The propeller shaft is placed in the middle of the reactor for symmetrical conditions; and no vibration is assumed during rotation.
- The propeller speed is 200 radians per minute 31.83 RPMs.
- The surface of the liquid lead is flat during the simulation; this condition is equal to assume a closed reactor.
- Lead temperature is assumed as 327.46°C (equal to 600.61K or 621.43°F). This is the lead melting point. The most important physical properties for this simulation, is liquid lead density equal to 10.66 g/cm<sup>3</sup>.
- Liquid lead is assumed as a heavy uncompressible fluid.
- During simulation, the reactor is assumed as an isothermal system.
- The tracer is injected into the reactor when the velocity of the fluid is stable.
- The simulation is done replacing and monitoring an edited lead volume, which is 1.25×10<sup>-4</sup>m<sup>3</sup>.
- Only one single volume is replaced during each simulation. And it is replaced at the beginning of the simulation (t=0).
- The tracer is injected always on the injected plane; in only one point for each simulation.
- Tracer is assumed as ideal; in other words, an original lead volume is substituted by other volume with the same physical properties. This method is frequently used by authors who work on physical and computer simulation [1-8] to evaluate fluid flow.

The control plane is divided in two semi-planes as shown in Figure 3. The first of them is the injection plane. Here all the nodes where the tracer is injected for each simulation are indicated. All of these are evaluated independently in order to find the best injection point. The second plane is the monitoring plane. Here are shown the points where the mixing efficiency is evaluated. The injection points have been placed on different positions all around in the injection plane to evaluate the influence of the reactor geometry and the propeller during rotating in order to identify death zones (zones with poor mixing) and zones where delaying on mixing is critical. The nearest points to the impeller are (Pi<sub>1</sub>, Pi<sub>4</sub>, Pi<sub>8</sub>, Pi<sub>14</sub>, and Pi<sub>18</sub>). These are placed along the shaft from the reactor surface to the blades. In the other hand the nearest injection points to the wall are (Pi<sub>6</sub>, Pi<sub>12</sub>, Pi<sub>12</sub>, Pi<sub>16</sub>, and Pi<sub>21</sub>). And the rest of the points were placed in central positions. Finally only one point was placed on the bottom to evaluate hydrodynamic behavior in this zone. Byung et al. (2004), used the residence time distribution method to analyze efficiency in a stirred tank. Hartmann and Derksen (2006) simulated dissolutions in a tank. Both authors validate these methods as appropriated to establish physical parameters to improve mixing. The parameter to evaluate mixing efficiency is the tracer diffusion in the entire reactor. This is done measuring the tracer concentration on each monitoring point.

### Monitoring points

The monitoring points are placed on a control plane at 180° from de injection plane. These points are used to save the tracer concentration (C<sub>tracer</sub>)

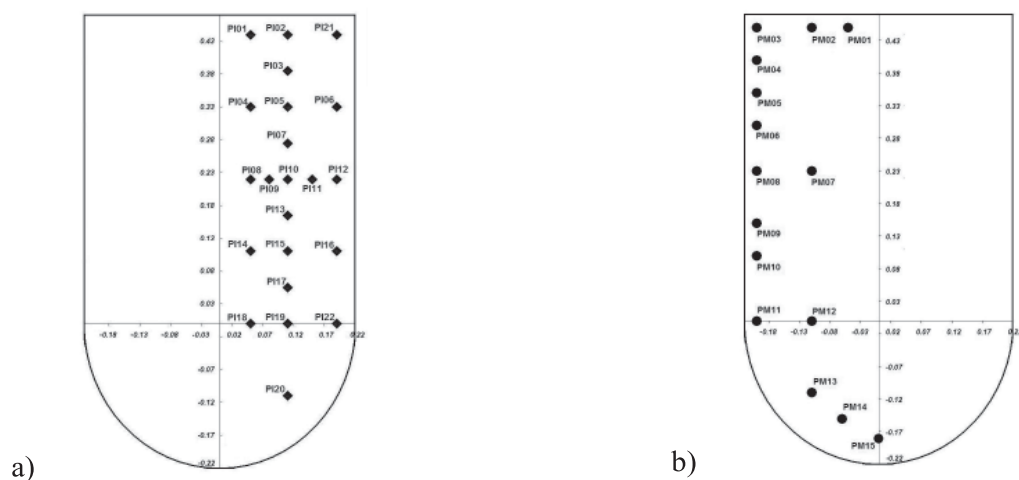


Fig. 3. Control planes with a) injection points b) with monitoring points  
Rys. 3. Panele kontrolne z a) punktami iniekcji; b) z punktami monitorującymi

at every step time ( $t+\Delta t$ ) during the simulation, in order to evaluate the mixing performance. Initially for a ( $t=0$ ) it is assumed the tracer concentration on each monitoring point is equal to zero ( $C_m=0$ ). Some of these points are placed in the middle of the reactor such as ( $pm_{22}$ ,  $pm_7$  &  $pm_{12}$ ); some others were placed near the walls such as ( $pm_{03}$ - $pm_{06}$ ) and ( $pm_{08}$ - $pm_{11}$ ). Finally the rest of these were placed in the bottom such as ( $pm_{13}$ ,  $pm_{14}$  &  $pm_{15}$ ).

Evaluation here is very important due to this region is considered as critical for mixing.

### Modeling

The equations solved are given by Navier-Stokes and continuity; which describe the motion of fluid substances. These equations arise from applying Newton's second law. The Navier-Stokes equations are nonlinear partial differential equations

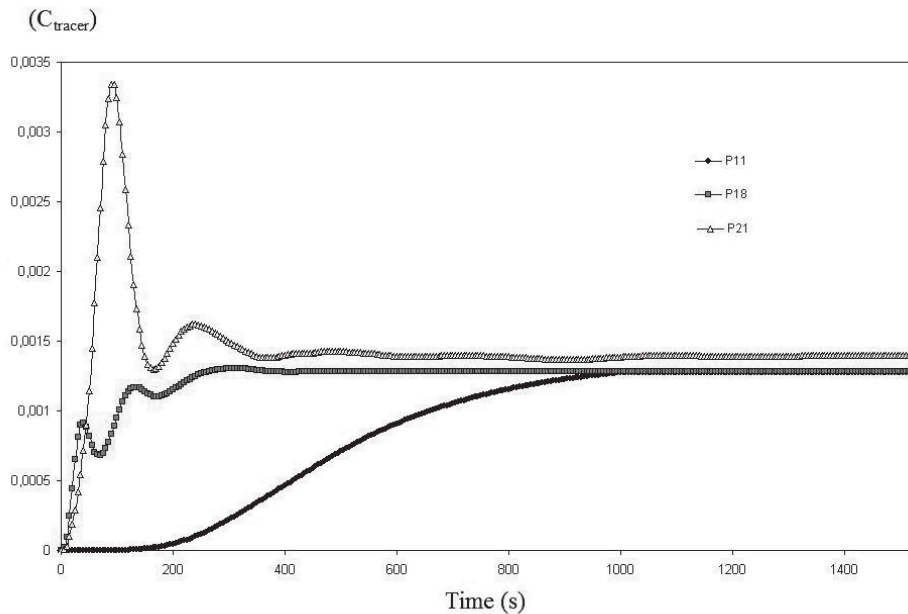


Fig. 4. Tracer concentration for the best, intermediate and worst injection points ( $P_{i_{18}}$ ,  $P_{i_{11}}$ ,  $P_{i_{21}}$  respectively)

Rys. 4. Stężenie pierwiastka znaczonego w najlepszych, średnich i najgorszych punktach iniekcji (odpowiednio  $P_{i_{18}}$ ,  $P_{i_{11}}$ ,  $P_{i_{21}}$ )

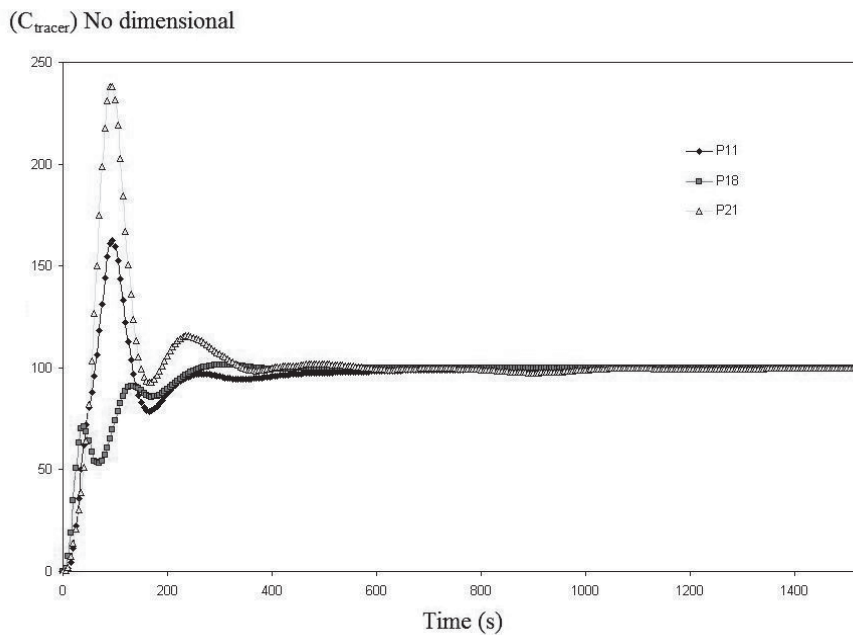


Fig. 5. Tracer concentration for the best, intermediate and worst injection points ( $P_{i_{18}}$ ,  $P_{i_{11}}$ ,  $P_{i_{21}}$  respectively) no dimensional curves

Rys. 5. Stężenie pierwiastka znaczonego w najlepszych, średnich i najgorszych punktach iniekcji (odpowiednio  $P_{i_{18}}$ ,  $P_{i_{11}}$ ,  $P_{i_{21}}$ ) bez krzywych wymiarowych

in almost every real situation. In some cases, such as one-dimensional flow, these equations can be simplified to linear equations. But nonlinearity makes most problems difficult or impossible to solve with conventional analysis due to the main contributor is the turbulence. The numerical solution of the Navier–Stokes equations for turbulent flows is complex, and due to the significantly different mixing-length scales that are involved in turbulent flow, the stable solution of these equations requires the definition of a fine mesh resolution during discretization in order to make feasible the computational treatment of data. Turbulence models such as the k-ε model, are used in practical computational fluid dynamics (CFD) applications when turbulent flows are modeled as is done in this work. The Navier–Stokes equations are strictly a statement of the conservation of momentum laws. In order to describe fluid flow in detail, more information is needed according with particular data and including boundary conditions. Some of the basic concepts involved are the conservation of mass and the conservation of energy related with an equation of state. A statement of the conservation of mass is achieved through the mass continuity equation, as is shown in equation (1). Navier-Stokes equations used are in 3 coordinates systems, here Cartesian is the system solved and equations are taken directly from the vector equations. The solution also implies the programming of the equations (2) to (4) using a numerical method. Here the velocity components (the dependent variables to be solved for) are typically named u, v, w. Simulation of stirring in a tank is a complex problem and many variables are involved; some authors as Hartmann and Derksen (2006), have include turbulence effects on solid-liquid suspensions to solve problems related with polymerization. Murthy et al. (2007) studied the hollow impeller effects to validate experimental fluid dynamics using CFD in order to evaluate the influence of the impeller speed.

$$\frac{\partial p}{\partial t} + \nabla \cdot (\rho v) = 0 \quad (1)$$

$$\rho \left( \frac{\partial u}{\partial t} + u \frac{\partial u}{\partial x} + v \frac{\partial u}{\partial y} + w \frac{\partial u}{\partial z} \right) = -\frac{\partial p}{\partial x} + \mu \left( \frac{\partial^2 u}{\partial x^2} + \frac{\partial^2 u}{\partial y^2} + \frac{\partial^2 u}{\partial z^2} \right) + \rho g_x \quad (2)$$

$$\rho \left( \frac{\partial v}{\partial t} + u \frac{\partial v}{\partial x} + v \frac{\partial v}{\partial y} + w \frac{\partial v}{\partial z} \right) = -\frac{\partial p}{\partial y} + \mu \left( \frac{\partial^2 v}{\partial x^2} + \frac{\partial^2 v}{\partial y^2} + \frac{\partial^2 v}{\partial z^2} \right) + \rho g_y \quad (3)$$

$$\rho \left( \frac{\partial w}{\partial t} + u \frac{\partial w}{\partial x} + v \frac{\partial w}{\partial y} + w \frac{\partial w}{\partial z} \right) = -\frac{\partial p}{\partial z} + \mu \left( \frac{\partial^2 w}{\partial x^2} + \frac{\partial^2 w}{\partial y^2} + \frac{\partial^2 w}{\partial z^2} \right) + \rho g_z \quad (4)$$

## Simulations

The model used for simulation was (k-ε) and the software used was Fluent 6.0. The tracer concentration was saved each step to be analyzed. The best injection point was (Pi<sub>18</sub>); and the worst injection point was (Pi<sub>21</sub>). Hydrodynamic behavior is studied saving the tracer concentration at each step (t+Δt) during simulation. Although is evident that the evolution on each monitoring point is particular. Sinusoidal curves are near propeller. Here the evolution of tracer concentration changes at every step during simulation due to the strong influence of vector velocities. In comparison; parabolic behavior is frequently observed near the walls. The evolution of tracer concentration is very slow here; and no strong fluctuations are presented due to these points are faraway of the propeller influence. Thus for long times, all the monitoring points tends to adopt the same averaged concentration. This means that the tracer has been homogeneously distributed inside the reactor. Tracer concentration values on all the monitoring points can be added and averaged in order to obtain a main value about the tracer concentration inside the reactor. Figure 4 shows these averaged curves to illustrate the general tracer concentration for the best, one intermediate and the worst injection points. Here it is possible to confirm (Pi<sub>18</sub>) is the best injection point. Its curve is sinusoidal, but it is quickly stabilized and the tracer variation is also quickly smoothed. No more than 450s. are required for the mixing. Also is possible to observe this curve never is upper the final tracer concentration. And the fluctuations are smoothed.

The point (Pi<sub>11</sub>) shows a moderate (intermediate) behavior. It is placed in the middle distance between the shaft and the wall. The curve is also sinusoidal although a very high excess of tracer concentration can be appreciated at the beginning. Nevertheless the variation on tracer concentration is stabilized as time goes. The time required for a good mixing is near to 850s. But the fluctuations are very high in comparison with the curve for the point (Pi<sub>18</sub>). This curve is upper the final tracer concentration value. This instability must be reduced; but additional stirring must be applied. The (Pi<sub>21</sub>) is the worst injection point. Here the time required for mixing is more than 1000 s. this curve is always below the final tracer concentration value due to the difficulty for the distribution on the bottom. The slope of this curve is low and the distribution is also slow.

Tracer concentration curves can be described in no dimensional representation by divided each value by the final concentration value. Figure 5 shows the no dimensional tracer concentration curves for

the previous shown in Figure 4. In consequence all the values will adopt the final tracer concentration as the 100 (%). And the distance from these curves to a horizontal is a parameter of the system instability. Here can also be appreciated that the curve for the point ( $pi_{18}$ ) is the first on reach homogeneity and also is with the minor fluctuations.

### Evaluation of injection points

Figures 6a to 6d show the tracer concentration pro-

files on the reactor for the best injection point ( $Pi_{18}$ ). These profiles were snapped for a one singled entire plane. The first of these was snapped at time ( $t=0$ ). Here the tracer is initially injected. Then on the rest of the figures it is possible to observe the evolution of tracer distribution. Figure 6b shows regions with an excess on tracer concentration but there are some others regions with a poor tracer concentration such as those near the bottom and the highest corner on the cylinder. Figure 6c shows a distribution nearly

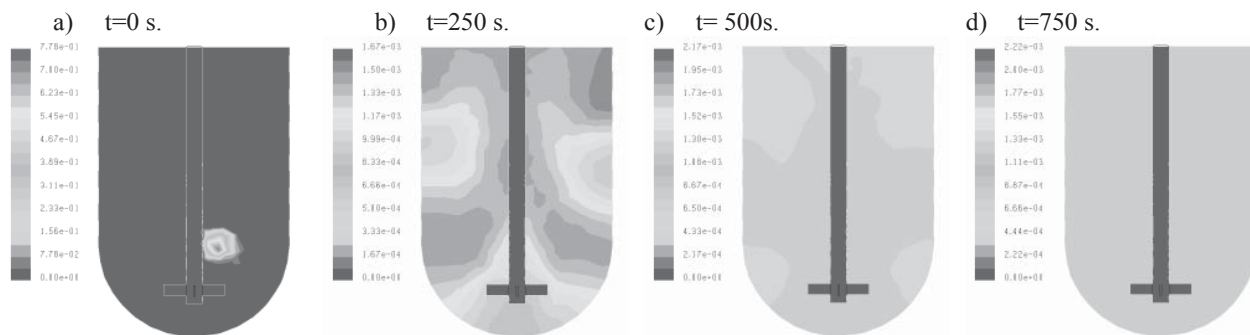


Fig. 6. Tracer concentration profiles at different simulation times for the injection point ( $Pi_{18}$ )

Rys. 6. Dane stężeń pierwiastków w różnym czasie symulacji dla punktu iniekcji ( $Pi_{18}$ )

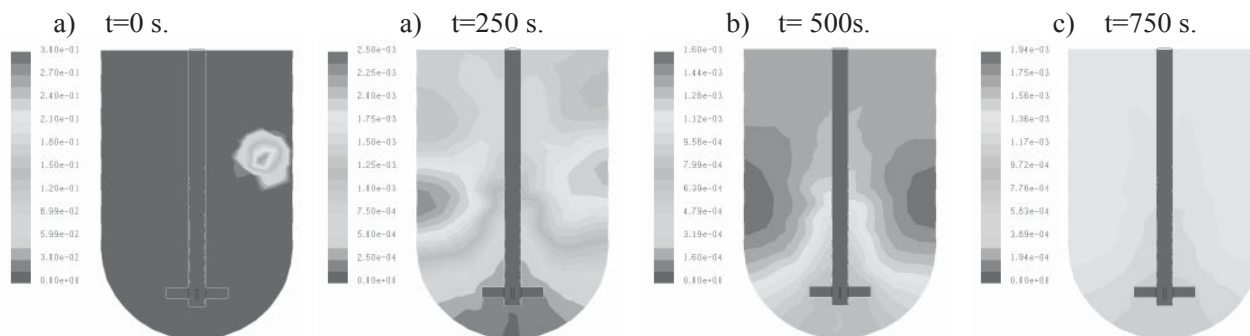


Fig. 7. Tracer concentration profiles at different simulation times for the injection point ( $Pi_{11}$ )

Rys. 7. Dane stężeń pierwiastków w różnym czasie symulacji dla punktu iniekcji ( $Pi_{11}$ )

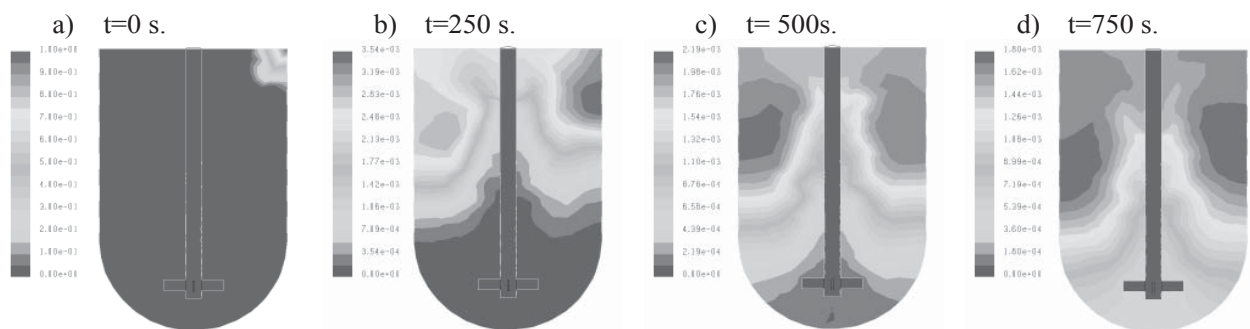


Fig. 8. Tracer concentration profiles at different simulation times for the injection point ( $Pi_{21}$ )

Rys. 8. Dane stężeń pierwiastków w różnym czasie symulacji dla punktu iniekcji ( $Pi_{21}$ )

homogeneous. There are four zones remaining with lower different tracer concentrations, these are near the cylinder top region; although the profile shows a very similar concentration in general terms. Figure 6d shows a profile with the same color in the entire reactor. It means that the all the liquid is perfectly mixed.

Figures 7a to 7d show the tracer concentration on the reactor for the intermediate point ( $P_{i11}$ ). In figure 7b the tracer has begun to be distributed on the reactor; but there are regions with a high and a low tracer concentration in the cylindrical section. Nevertheless big zones with low tracer concentration can be appreciated in the bottom. In Figure 7c, high tracer concentrations remain on the cylindrical section near the walls; the tracer has been introduced in the reactor bottom but the profile is still being no homogeneous. Finally, Figure 7d shows a more homogeneous distribution of the tracer all around the reactor, zones with very high and low tracer concentrations have disappeared and the profile looks more homogeneous. But this distribution remains with a low efficiency in comparison with that shown in figures 6a to 6d; and longer times for stirring are necessary to obtain a good mixing.

Figures 8a to 8d show the tracer concentration on the reactor for the worst injection point ( $P_{i21}$ ). Here the tracer is injected in a point near the reactor surface and near the wall as is shown in Figure 8a. This point is placed faraway from the impeller and the influence of the rotational movement is weak in consequence the tracer distribution is very slow as is shown in Figures 8b and 8c. Here the tracer begins to appear in regions of the cylindrical section. Nevertheless huge regions without tracer can be appreciated into the reactor bottom due to the slow diffusion. The final profile on Figure 8d shows a heterogeneous distribution of the tracer. The meaning is that the mixing efficiency is poor.

## Conclusions

Tracer concentration in monitoring points near the propeller is strongly influence by the rotational speed and strong fluctuations of the tracer concentration are observed. The highest saturations are in this region; nevertheless the tracer excess is distributed quickly due to the stirring.

Tracer concentration evolution is different on each monitoring point as a function of its position on the reactor and the injection point analyzed. Sinusoidal curves for tracer concentration are evidence of the instability of the system; this tracer must be homogeneously distributed for mixing. When these are smoothed the tracer concentration tends to be homogeneous.

Evolution of tracer concentration is a feasible parameter to evaluate mixing. Moreover understanding the hydrodynamic inside the stirred lead reactor is very important to improve its performance.

The selection of the best injection point is very important to reduce working times and avoid unnecessary work.

According with the simulations done; it is possible to affirm that the tracer must be injected near the impeller in order to profit the stirring forces. Therefore the injection of tracer on points near the surface or reactor wall must be avoided due to these are with the most delayed mixing times.

## Acknowledgments

The authors wish to thanks to: Consejo Nacional de Ciencia y Tecnología (CONACyT), Instituto Tecnológico Autónomo de México (ITAM), Instituto Politécnico Nacional (IPN-ESIQIE) and special mention to: Asociación Mexicana de Cultura.

Received January 6, 2015; reviewed; accepted March 17, 2015.

## Literatura - References

1. Bailey C., Kumar S., Patel M. et al. "Comparison between CFD and measured data for the mixing of lead bullion". *Second International Conference on CFD in Minerals and Process Industries CSIRO, Melbourne, Australia 6-8 December (1999)* p. 351–356.
2. Byung S., Choi, and Bin Wan, Susan Philyaw, Kuman Dhanasekharan and Terry A. Ring, "Residence Time Distributions in a Stirred Tank: Comparison of CFD Predictions with Experiment", *Ind. Eng. Chem. Res.* (2004), vol. 43, p. 6548–6556.
3. Debangshu Guha, P.A. Ramachandran and M.P. Dudukovic, *Flowfield of suspended solids in a stirred tank reactor by Lagrangian tracking*, *Chemical Engineering Science* vol. 62 (2007), p. 6143–6154.
4. FengWang, Zai-Sha Mao, Yuefa Wang and Chao Yang, "Measurement of phase holdups in liquid-liquid-solid three-phase stirred tanks and CFD simulation", *Chemical Engineering Science* vol. 61 (2006), p. 7535–7550.
5. Hartmann H., Derksen J.J, and Van Den Akker, "Numerical simulation of a dissolution process in a stirred tank reactor", *Chemical Engineering Science* vol. 61, (2006) p. 3025–3032.
6. Huang Si, Abdulmajeed Mohamad and K. Nandakumar, "Numerical Analysis of a Two-Phase Flow and Mixing Process in a Stirred Tank", *International Journal of Chemical Reactor Engineering*, vol. 6 2008 Article A38.
7. Koh P.T.L. and Xantidis f., "CFD Modelling in the scale-up of a stirred reactor for resin beads", *Second International Conference on CFD in Minerals and Process Industries CSIRO, Melbourne, Australia 6-8 December (1999)* p. 369–374.
8. Murthy B.N., Deshmukh N.A., Patwardhan A.W. and Joshi J.B., "Hollow self-inducing impellers: Flowvisualization and CFD simulation", *Chemical Engineering Science* vol. 62, (2007), p. 3839–3848.
9. Zhong Zhang and Guanrong Chen, "Liquid mixing enhancement by chaotic perturbations in stirred tanks", *Chaos, Solitons and Fractals* vol. 36, (2008), p. 144–149.

### Zwiększenie wydajności łączenia w Reaktorze Mieszalnikowym dla odzysku ołowiu przy użyciu symulacji komputerowej

Recykling pomaga zredukować ryzyko i szkody związane ze środowiskiem. Ciekły ołów z baterii odnawiany jest w reaktorze mieszalnikowym okresowym. Niemniej jednak, ważne jest by tak ustawić parametry, żeby ocenić skuteczność mieszania, a co za tym idzie, zwiększyć wydajność w praktykach przemysłowych. Następnie w artykule znajdujemy najlepsze miejsce do iniekcji przy użyciu symulacji dynamiki wodnej w płynie w reaktorze mieszalnikowym ołowiu, dzięki obserwacji ruchów wprowadzonego pierwiastka znaczonego. Różne punkty iniekcji zostały sprawdzone i monitorują pierwiastek znaczony w grupie punktów znajdujących się w reaktorze by zweryfikować mieszanie. Z założenia pierwiastek jest idealny (z tymi samymi właściwościami fizycznymi co ołów). Reaktor jest wsadowy z dwoma geometrycznymi sekcjami – jedną z cylindryczną obudową i drugą o półsferycznym dnie. Wirnik napędza mieszanie ołowiu w wale posiadającym cztery płaskie ostrza. Punkty monitorujące mają uśrednione stężenie pierwiastka w taki sposób, aby ocenić wydajność w całym reaktorze. Wreszcie, jednym z kryteriów wprowadzonych dla odpowiedniej oceny wydajności jest również niezmienność stężenia pierwiastka monitorującego.

Słowa kluczowe: mieszanie ołowiu, ocena wydajności mieszania, stężenie pierwiastka, obliczeniowa mechanika płynów (CFD)